A robust finite element modelling approach to conjugate heat transfer in flexible elastic tubes and tube networks.

Alberto Coccarelli and Perumal Nithiarasu*

Biomedical Engineering and Rheology Group
Zienkiewicz Centre for Computational Engineering
College of Engineering, Swansea University, Swansea SA2 8PP, UK

Abstract

In this work, heat transfer between fluid flow in elastic tubes and external environment is modelled using a robust finite element approach. The transport of energy is coupled to fluid flow that is linked to the pressure and cross sectional area variations of the tube. The novel model developed is applied to flow and heat transfer in elastic tubes with different geometric and material properties. The effects of reflections due to discontinuities and bifurcations in the tubes are also investigated. To determine the heat transport by conduction in the elastic walls, a radial heat conduction model is also incorporated. The coupled flow equations are solved using the locally conservative Galerkin (LCG) finite element method, which provides an explicit element-wise conservation of fluxes. Several simulations have been performed for different parameter variations to understand the relevant aspects of heat transfer in flexible elastic tubes. The results show that small temperature fluctuations are possible, inline with the pulsatile flow boundary conditions. It is also observed that increased flexibility of tubes leads to better heat transfer between the fluid and the wall. The results clearly indicate that any flow reflections also increase the heat transfer between the fluid and the wall.

KEY WORDS: elastic tubes, conjugate heat transfer, finite element, blood vessels, bioheat transfer.

Nomenclature

A	Cross sectional area
A_{ex}	External surface area
A_{in}	Internal surface area
A_o	Stress free cross sectional area
c	Intrinsic wave speed
c_{max}	Maximum intrinsic wave speed
c_p	Specific heat at constant pressure of fluid
c_s	Specific heat at constant pressure of wall

*Correspondance to Professor P Nithiarasu, e-mail: P.Nithiarasu@swansea.ac.uk

$\mathbf{D}_{eT}$	Element matrix for temperature diffusion in fluid
E	Youngs modulus of wall material
E_s	Specific energy
e	Internal energy
$\mathbf{f}_{\Gamma e}$	Boundary terms at element boundaries
$\mathbf{F}$	Convective and Taylor Galerkin fluxes
$\bar{\mathbf{G}}$	Diffusion vector
$\mathbf{H}$	Jacobian matrix
h	Pipe wall thickness
h_{ex}	External heat transfer coefficient
h_{in}	Internal heat transfer coefficient
$\mathbf{I}$	Identity matrix
$\mathbf{K}_e$	Element matrix for convection and Taylor Galerkin terms
$\mathbf{K}_{eT}$	Element matrix for temperature convection and Taylor Galerkin terms
k	Thermal conductivity of fluid
k_s	Thermal conductivity of solid
$\mathbf{L}$	Eigen matrix
$\mathbf{L}_e$	Element matrix of source terms
l	Total length of a tube
l_i	Eigen vectors
$\mathbf{M}_e$	Element mass matrix
$\mathbf{M}_{eT}$	Element mass matrix for temperature
$\mathbf{N}$	Shape function matrix
N	Number of daughter vessels
P	Parent vessel
p	Pressure
$\bar{p}$	Given pressure value
p_{ext}	External pressure
$\mathbf{Q}$	Jacobian of source
Q	Flow rate
q_v	Heat generation
$\mathbf{q}_{\Gamma e}$	Element boundary term for energy equation
R	Inner radius of a tube
R_t	Terminal reflection coefficient
r	Radial direction
r_{in}	Internal radius
r_{ex}	External radius
$\bar{\mathbf{S}}$	Source vector
T	Temperature
T_{ex}	Atmospheric temperature

T_s	Outer wall temperature
T_w	Inner wall temperature
t	Time
$\bar{\mathbf{U}}$	Primitive variable vector of area and velocity
u	Velocity
x	Cartesian coordinate
$\dot{W}_{shear}$	Loss due to viscous effect
$\dot{W}_{wall}$	Work by wall forces
w_1, w_2, w_3	Characteristic variables

Greek letters

α	Thermal diffusivity
β	Material parameter of wall
Δt	Time step
Δx	Element size
$\Delta\mathbf{T}$	$= \mathbf{T}^{n+1} - \mathbf{T}^n$, Nodal values of difference in T
$\Delta\mathbf{U}$	$= \mathbf{U}^{n+1} - \mathbf{U}^n$, Nodal values of difference in $\bar{\mathbf{U}}$
$\bar{\mathbf{\Lambda}}$	Eigen value matrix
λ	Eigen value
μ	Viscosity
$\dot{\Phi}_{conv}$	Heat convection flux
$\dot{\Phi}_{diff}$	Heat diffusion flux
ρ	Fluid density
σ	Poisson's ratio
τ	Shear stress

1 Introduction

One-dimensional flow modelling in elastic tubes and tube networks has tremendously improved our understanding of human circulatory system. Although a large number of works on blood circulation has been published in the last thirty years [1]–[18], the focus of these works has been limited to isothermal flow. However, understanding energy transport in circulatory systems is vital for applications such as hypothermia and hyperthermia [19, 20, 21, 22]. Thus, a comprehensive model to study the relationship between fluid flow and temperature in flexible tubes is very relevant and important in bioheat transfer problems.

The literature available in the area of energy transport in flexible tubes or circulatory systems is very limited. The work of Craciunescu and Clegg [23] analysed the effect of blood velocity pulsations on temperature field. They obtained some important results on the relationship between the pulsating axial velocity and temperature profile and the effect of the Womersley number. However,

blood vessels in this study are treated as rigid tubes and thus the effects of area variations are not accounted. Thus the results obtained in their study have limitations. Ying et al. [24] proposed a thermo-fluid model for circulation in the upper limb, which involves arteries, capillaries, and veins. Here, the temperature is evaluated along the network by considering the effects of blood flow rate, transmural pressure, cross-sectional area and elasticity. However, this model is not comprehensive as it has not fully accounted for reflections due to variations in vessel topology and properties. Although the comprehensive models for temperature transport in the circulatory systems are limited, a large number of robust models are available for isothermal flow in circulatory systems [10, 11]. Therefore, in the present work we used such existing isothermal models to build a non-isothermal model to comprehensively describe not only the heat transfer in the fluid but also through the solid wall.

In the present work, the coupled one-dimensional equations of flow and energy are expressed in terms of a tube cross-sectional area, velocity, pressure and temperature. To relate pressure to area, a non-linear elastic wall law is used. The viscous effects are modelled using Poiseuille flow assumptions. The physics of the problem may be described as follows. The fluid in the flexible tube exchanges heat to the wall along its path in the axial direction. This results in variable axial velocity, pressure and temperature in space and in time. These variables are then coupled to the wall heat condition via an inner and outer wall thermal conditions.

The numerical scheme used for solving the set of flow and temperature equations is the explicit form of locally conservative Taylor Galerkin method (LCG) [25, 26]. Local method implies that spatial integration is performed element by element, which eliminates the need for large matrix inversions. Besides, this choice is particularly suitable for including discontinuities and vessel branching points, where multiple nodes occupy the same spatial location. The conduction problem in the walls along the radial direction is solved using a standard implicit finite difference method.

To demonstrate the proposed energy transport model, relationships between temperature field, material properties and geometry are extensively studied for a single tube first. The model is also applied to complex systems that accounts for discontinuities and vessel branching, so that the effects of reflections can be analyzed. As the governing equations are hyperbolic and the flow is subsonic, boundary conditions for primitive variables are required at the inlet and at the exits. The nature of the problem allows one to calculate the characteristic variables and these variables may be used for prescribing boundary conditions at the inlet and exit and also for determining the conditions at discontinuities and bifurcations.

The paper is organised into following sections. The section that follows describe the detailed mathematical formulation of the problem. Section 3 provides a brief summary of the finite element formulation and the results are discussed in Section 4. Finally, Section 5 derives some conclusions.

2 Mathematical formulation of the problem

The variables considered in the system are cross sectional area (A), the average values of velocity (u), fluid pressure (p) and temperature (T) over the cross section (see Figure 1). The density (ρ)

of the fluid and wall are assumed to be constant due to the incompressible nature of the materials assumed. The viscosity (μ) of the fluid is also assumed to be a constant. Due to the one-dimensional nature of the model, the shear stress is evaluated using Poiseuille's flow assumption, i.e.,

$$\frac{d\tau}{dx} = -\frac{8\mu Q(x,t)}{\pi R^4} = -\frac{8\pi\mu u(x,t)}{A(x,t)} \tag{1}$$

where $Q = Au$ is the volume flow rate averaged over a cross-section. Due to the simplified assumptions, the model is not valid for cases in which flow is non-Newtonian or turbulent. In order to reduce the number of parameters, specific heat (c_p) and thermal conductivity (k) of the materials are also assumed to be constant.

The full problem may be described by four equations: the conservation laws of mass, momentum and energy and a constitutive elastic wall model to define the relationship between the fluid pressure and the cross section area. Following existing literature [27], the equations of mass and momentum for an elastic vessel may be written as

$$\frac{\partial A(x,t)}{\partial t} + \frac{\partial Q(x,t)}{\partial x} = 0 \tag{2}$$

$$\frac{\partial u(x,t)}{\partial t} + u(x,t)\frac{\partial u(x,t)}{\partial x} + \frac{1}{\rho}\frac{\partial p(x,t)}{\partial x} - \frac{1}{\rho}\frac{\partial \tau(x,t)}{\partial x} = 0 \tag{3}$$

It is important to remind the reader that these equations are valid for an infinitesimal cylindrical element of area A and length dx. For relating pressure and cross sectional area, a non linear relation used by Formaggia et al. [28] and Olufsen et al. [29] is employed, i.e.,

$$p(x,t) = p_{ext} + \beta\left(\sqrt{A(x,t)} - \sqrt{A_0(x)}\right) \tag{4}$$

where p_{ext} is the external pressure acting on the walls of the tube, A_0 is the unstressed cross-section area and β is the characteristic property of elastic material and it is defined as

$$\beta = \frac{\sqrt{\pi}hE}{A_0(1-\sigma^2)} \tag{5}$$

where E is Young's modulus of the wall material, h is the wall thickness (see Figure 1) and σ the Poisson ratio of the wall material. By inserting Equations (1) and (4) in to Eq. (3), it is possible to express the momentum equation only in terms of area and velocity:

$$\frac{\partial u(x,t)}{\partial t} + u(x,t)\frac{\partial u(x,t)}{\partial x} + \frac{\beta}{2\rho\sqrt{A(x,t)}}\frac{\partial A(x,t)}{\partial x} - \frac{1}{\rho}\frac{\partial \tau(x,t)}{\partial x} = 0 \tag{6}$$

Considering the 1D elastic vessel shown in Figure 1, the integral balance of energy may be written as:

$$\begin{aligned}\dot{\Phi}_{conv}(t) =& \dot{W}_{wall}(t) + \dot{W}_{shear}(t) + \dot{\Phi}_{cond}(0,t) - \dot{\Phi}_{cond}(l,t) \\ &+ \rho Q(l,t)\left(E_s(l,t) + \frac{p(l,t)}{\rho}\right) - \rho Q(0,t)\left(E_s(0,t) + \frac{p(0,t)}{\rho}\right) \\ &+ \rho \frac{\partial}{\partial t}\int_0^l A(x,t)E_s(x,t)\,dx\end{aligned} \tag{7}$$

where E_s represents the specific energy of the fluid obtained as a sum of the specific internal energy and the kinetic energy ($E_s = e + \frac{u^2}{2}$), $\dot{\Phi}_{cond}$ is the conduction fluxes in the fluid, while $\dot{\Phi}_{conv}$, $\dot{W}_{wall}$ and $\dot{W}_{shear}$ are respectively the thermal flux exchanged by convection, integral quantities along the tube due to fluid forces on the walls and viscous losses. After simplification, the differential one-dimensional energy conservation equation for an infinitesimal tube (without considering viscous effects) may be written as,

$$\frac{\partial T(x,t)}{\partial t} + u(x,t)\frac{\partial T(x,t)}{\partial x} - \alpha\frac{\partial^2 T(x,t)}{\partial x^2} = \frac{2h_{in}}{\rho c_p\sqrt{A(x,t)/\pi}}(T_w(x,t) - T(x,t)) \tag{8}$$

where α is the thermal diffusivity of the fluid, h_{in} is the heat transfer coefficient at the inner surface of the wall and T_w is the inner wall temperature. The full system of equations composed of Equations (2), (6) and (8) and it is non-linear and the first and second equations are strongly coupled. However, the mass and momentum conservation equations do not depend on the temperature. Thus, it is possible to split the solution process into two steps: in the first step one can calculate the velocity, cross sectional area and pressure using Equations (2) and (6) before computing the temperature in the second step. In order to asses the heat transfer between the inner fluid and the external environment, a one-dimensional heat conduction equation in the radial direction is used, i.e.,

$$\rho_s c_s \frac{\partial T(r,t)}{\partial t} - k_s \frac{1}{r}\frac{\partial}{\partial r}\left(r\frac{\partial T(r,t)}{\partial r}\right) - q_v = 0 \tag{9}$$

In the above equation, r is the radial coordinate, q_v is the volumetric heat generation (assumed to be zero in the present study) and ρ_s, c_s, k_s are respectively the density, the specific heat and the thermal conductivity of the wall material. The system of equations is completed by appropriate initial and boundary conditions.

3 Solution procedure

3.1 Characteristic system

In order to assign boundary conditions and to apply the Taylor Galerkin method, it is convenient to write the whole system in a linearized de-coupled form. In Formaggia et al. [3] and Sherwin et al. [27], the system composed of mass and momentum conservation equations are written in a quasi linear form. Incorporating the energy equation requires a similar procedure. The system of

Equations (2), (6) and (8) may be written as

$$\frac{\partial \bar{\mathbf{U}}}{\partial t} + \mathbf{H}\frac{\partial \bar{\mathbf{U}}}{\partial x} + \frac{\partial \bar{\mathbf{G}}}{\partial x} = \bar{\mathbf{S}} \tag{10}$$

with:

$$\bar{\mathbf{U}} = \begin{bmatrix} A \\ u \\ T \end{bmatrix}; \quad \mathbf{H} = \begin{bmatrix} u & A & 0 \\ \frac{\beta}{2\rho\sqrt{A}} & u & 0 \\ 0 & 0 & u \end{bmatrix}; \quad \bar{\mathbf{G}} = \begin{bmatrix} 0 \\ 0 \\ -\alpha\frac{\partial T}{\partial x} \end{bmatrix} \quad \text{and} \quad \bar{\mathbf{S}} = \begin{bmatrix} 0 \\ -8\pi\frac{\mu}{\rho}\frac{u}{A} \\ \frac{2h_{in}}{\rho c_p\sqrt{A/\pi}}(T_w - T) \end{bmatrix}$$

where $\bar{\mathbf{U}}$, $\bar{\mathbf{G}}$ and $\bar{\mathbf{S}}$ are the vectors of primitive variables, the diffusive and source terms, while $\mathbf{H}$ is the Jacobian matrix of the convective term for the primitive variables. If diffusion and sources are considered negligible ($\frac{\partial \bar{\mathbf{G}}}{\partial x} = 0$ and $\bar{\mathbf{S}} = 0$), the characteristic variables of Equation (10) may be determined.

Eigenvalues ($\bar{\mathbf{\Lambda}}$) and eigenvectors (l_i) of the characteristic system are evaluated respectively by solving $|\bar{\mathbf{\Lambda}}\mathbf{I} - \mathbf{H}| = 0$ and $l_i\mathbf{H} = \lambda_i l_i$ [30]. In this case all eigenvalues associated to matrix H are real numbers, i.e.,

$$\bar{\mathbf{\Lambda}} = \begin{bmatrix} \lambda_1 \\ \lambda_2 \\ \lambda_3 \end{bmatrix} = \begin{bmatrix} u + c \\ u - c \\ u \end{bmatrix} \tag{11}$$

where c is the intrinsic wave speed associated with the flexible wall material, expressed as

$$c = \sqrt{\frac{\beta\sqrt{A}}{2\rho}} \tag{12}$$

Eigenmatrix is:

$$\mathbf{L} = \begin{bmatrix} c/A & 1 & 0 \\ -c/A & 1 & 0 \\ 0 & 0 & 1 \end{bmatrix} \tag{13}$$

The characteristic variables are defined as

$$dw_i = l_i\bar{\mathbf{U}} \tag{14}$$

and integration gives,

$$\begin{bmatrix} w_1 \\ w_2 \\ w_3 \end{bmatrix} = \begin{bmatrix} u + 4c \\ u - 4c \\ T \end{bmatrix} \tag{15}$$

By rearranging the above equations, it is possible to express the primitive variables in terms of the characteristic variables as

$$A = \frac{(w_1 - w_2)^4}{1024}\left(\frac{\rho}{\beta}\right)^2, \quad u = \frac{1}{2}(w_1 + w_2) \quad \text{and} \quad T = w_3 \tag{16}$$

Writing Equation (10) in terms of characteristic variables allows one to understand how information is transported in the domain considered. The physical interpretation of the first and second characteristic variables is that pressure and velocity wave fronts propagate forwards (towards exit) at a speed of $u + c$ and backwards (towards inlet) at $u - c$. A wave front may be considered to be a particular point on a pulse [31](for example, the peak or the foot). The third characteristic variable instead, has the eigenvalue equal to the velocity u. Thus it means that the temperature is a property transported by the flow with the effective velocity of the fluid u.

3.2 Numerical scheme

In this section, a brief overview on the numerical method employed is provided. The details on the isothermal formulation is discussed in detail in reference [10]. Equation (10) requires a scheme with a stabilization term to obtain a stable solution. Thus, in this study the Locally conservative Taylor Galerkin method is used, which is the finite element equivalent of Lax - Wendroff stabilization in finite difference discretization. Using this method, the semi-discrete form of Equation (10) may be written as,

$$\begin{aligned}\frac{\bar{\mathbf{U}}^{n+1} - \bar{\mathbf{U}}^n}{\Delta t} = &-\left[\mathbf{H}^n \frac{\partial \bar{\mathbf{U}}^n}{\partial x} + \frac{\partial \bar{\mathbf{G}}^n}{\partial x} - \bar{\mathbf{S}}^n\right] \\ &+ \frac{\Delta t^2}{2}\left\{\frac{\partial}{\partial x}\left[\mathbf{H}^n\left(\mathbf{H}^n \frac{\partial \bar{\mathbf{U}}^n}{\partial x} - \bar{\mathbf{S}}^n\right)\right] - \mathbf{Q}^n\left(\mathbf{H}^n \frac{\partial \bar{\mathbf{U}}^n}{\partial x} + \frac{\partial \bar{\mathbf{G}}^n}{\partial x} - \bar{\mathbf{S}}^n\right)\right\}\end{aligned} \tag{17}$$

Applying LCG method, Equation (17) may be written as[25, 26]:

$$\begin{aligned}\int_{\Omega_e} \mathbf{N}^T \Delta \bar{\mathbf{U}}^{n+1} dx = &-\Delta t \int_{\Omega_e} \mathbf{N}^T \left[H^n \frac{\partial \bar{\mathbf{U}}^n}{\partial x} + \frac{\partial \bar{\mathbf{G}}^n}{\partial x} - \bar{\mathbf{S}}^n\right] dx \\ &+ \frac{\Delta t^2}{2} \int_{\Omega_e} \mathbf{N}^T \left\{\frac{\partial}{\partial x}\left[\mathbf{H}^n\left(\mathbf{H}^n \frac{\partial \bar{\mathbf{U}}^n}{\partial x} - \bar{\mathbf{S}}^n\right)\right] + \mathbf{Q}^n\left(\mathbf{H}^n \frac{\partial \bar{\mathbf{U}}^n}{\partial x} + \frac{\partial \bar{\mathbf{G}}^n}{\partial x} - \bar{\mathbf{S}}^n\right)\right\} dx\end{aligned} \tag{18}$$

The evaluation of Equation (18) for mass or momentum equations have been discussed by Mynard and Nithiarasu [10] in detail. The final discrete form of Equation (18) may now be written as

$$[\mathbf{M}_e]\{\Delta \mathbf{U}\}^{n+1} = \Delta t \left([\mathbf{K}_e]\{F\}^n + [\mathbf{L}_e]\{\mathbf{S}\}^n + \mathbf{f}_{\Gamma_e}{}^n\right) \tag{19}$$

where $[\mathbf{M}_e]$, $[\mathbf{K}_e]$ and $[\mathbf{L}_e]$ are respectively the element mass matrix, the coefficient matrix for convection, Taylor-Galerkin and source terms for the coupled continuity and momentum equations. These element matrices of the system of equations is solved on individual elements, independent

of surrounding elements. Information is transmitted between elements via the numerical flux term ($\mathbf{f}_{\Gamma_e}$) that is imposed along the boundaries of each element[10, 25]. As mentioned previously, the energy equation may be decoupled from the other equations due to one way nature of the coupling. If decoupled, the energy Equation (18) may be discretized as

$$[\mathbf{M}_{eT}]\{\Delta\mathbf{T}\}^{n+1} = \Delta t\{([\mathbf{K}_{eT}] + [\mathbf{D}_{eT}] + [\mathbf{L}_{eT}])\{\mathbf{T}\}^n + \mathbf{q}^n_{\Gamma_e}\} \tag{20}$$

where the matrix $[\mathbf{D}_{eT}]$ is the coefficient matrix for diffusion and $\mathbf{q}_{\Gamma_e}$ is the numerical conduction flux exchanged between two adjacent elements. The time step restrictions of the numerical scheme employed may be computed using the condition [10],

$$\Delta t = 0.9\frac{\Delta x_{min}}{c_{max}} \tag{21}$$

For the problem of heat conduction in the wall, the standard forward Euler method is used. The method uses the central difference scheme for spatial discretization and a first order discretization for the time term. Thus, the discrete form of Equation (9) for a node i may be written as

$$\begin{aligned} &T^n_{i-1}\frac{\Delta t k_s}{\rho_s c_s r_i}(-\frac{r_i}{\Delta r^2} + \frac{1}{2\Delta r}) + T^n_i(1 + \frac{2\Delta t k_s}{\rho_s c_s \Delta r^2}) - T^n_{i+1}\frac{\Delta t k_s}{\rho_s c_s r_i}(\frac{r_i}{\Delta r^2} + \frac{1}{2\Delta r}) \\ &= \frac{\Delta t}{\rho_s c_s}q_v + T^{n-1}_i, \qquad i = 1, 2, ..m \end{aligned} \tag{22}$$

Since the matrix of the linear system is tridiagonal, Thomas algorithm is used to solve the above system.

3.3 Boundary conditions

For the system of discrete equations discussed in the previous subsections, inlet and outlet variables may be imposed by calculating the characteristic variables. This is one of the best ways of imposing the correct boundary conditions. For the inlet node the forward characteristic (w_1) variable may be calculated if forward pressure is prescribed (that is strictly linked with forward area). From Equation (15), we may write

$$w^{n+1}_{1in} = w^0_2 + 4\sqrt{\frac{2}{\rho}}\sqrt{(\bar{p}^{n+1} - p_{ext}) + \beta\sqrt{A_0}} \tag{23}$$

where w^0_2 is the initial value of w_2 and is also equal to the value of w_2 at any time if no backward-running waves reach the inlet. In the above equation, $\bar{p}^{n+1}$ is the given pressure boundary condition at the inlet. The backward characteristic variable (w_2) at the inlet may be evaluated via linear extrapolation in the $x - t$ plane, i.e.,

$$w^{n+1}_2|_{x=x_0} = w^n_2|_{x=x_0+\lambda^n_2\Delta t} \tag{24}$$

It is now possible to evaluate the primitive variables A and u at the inlet node using Equation

(16). In the same way, it is possible to assign the boundary condition to the exit node of the domain. Calculation of the backward characteristic variable on the exit node may also be performed by prescribing reflections at the exit. In this case, the change in the incoming characteristic variable could be determined from the change in the outgoing characteristic variable. For a wave front travelling in $+x$ direction the terminal reflection coefficient is,

$$R_t = \frac{w_2^{n+1} - w_2^0}{w_1^{n+1} - w_1^0} \tag{25}$$

The value of w_1 for the next time step ($t = n+1$)may be determined via extrapolation, whereas w_1^0 and w_2^0 are the initial values of the characteristic variables. The unknown (w_2^{n+1}) may then be determined by simply rearranging Equation (25) if the reflection coefficient is known, i.e.,

$$w_2^{n+1} = w_2^0 - R_t(w_1^{n+1} - w_1^0) \tag{26}$$

Further details on the flow boundary conditions may be obtained from relevant published work [10, 11]. The boundary conditions for the energy equations are discussed next. The constant temperature conditions at the inlet and exit is straightforward to prescribe. For conduction in the solid, the boundary conditions are prescribed after obtaining the solution in the fluid domain. In the present work, for the interface node between the fluid and wall either constant wall or convective boundary conditions are assumed. For the outer surface node connected to the atmosphere, only convective boundary conditions are imposed. The inner and outer wall convective boundary conditions are given respectively as

$$h_{in}A_{in}(T_{in} - T_s(r_{in})) = -kA_{in}\frac{\partial T_s}{\partial r}|_{r_{in}} \tag{27}$$

and

$$h_{ex}A_{ex}(T_s(r_{ex}) - T_{ex}) = -kA_{ex}\frac{\partial T_s}{\partial r}|_{r_{ex}} \tag{28}$$

At branching points and discontinuities, the work of Mynard and Nithiarasu is followed [10].To transmit information between co-located nodes, the characteristic variables are used, in addition to standard flow conditions. If we consider a parent vessel P with N daughter vessels, each of the $N + 1$ co-located nodes are treated as boundaries and the boundary conditions will be set using upstream and downstream information. There are therefore $3(N+1)$ unknowns and as many equations required to solve the system. For example, in a bifurcation there are one parent vessel and two daughter vessels. Thus, we need a total of nine equations to determine the primitive variable values at three nodes. The conservation of mass gives one equation, pressure continuity between parent and daughter vessels gives two more equations, three characteristic flow variables at three nodes give three more equations. This is normally sufficient to carryout the flow calculations as explained in [10]. The set of non-linear equations resulting from the application of conditions at discontinuities is solved using the Newton -Raphson method [32].

To add the energy equation, we need to have three more equations. The characteristic variable

for temperature from Equation 15 may be rewritten as

$$w_{3p} = T_p \quad \text{for a forward moving flow and} \quad w_{3i} = T_i \quad \text{for a backward moving flow} \tag{29}$$

where subscripts p and i indicate parent and daughter vessels respectively.

Thus, for a forward moving wave, characteristic variable at the parent node may be extrapolated using an equation similar to Equation24 but for w_3. This will give the temperature value at the parent node (Equation 29). The energy conservation and temperature continuity dictates that the temperature at the parent node is equal to temperature at daughter nodes. This is due to the fact that for a forward moving wave temperature values at the daughter vessel nodes are identical.

If the wave is travelling in the backward direction towards the parent node, identical temperatures in daughter nodes are not guaranteed. Thus the characteristic variables at the daughter notes should be extrapolated to obtain the temperature values at these nodes(Equation 29). Once these values are determined, energy conservation may be applied to determine the temperature value at the parent node.

4 Results and discussions

In the following subsections the energy transport results obtained are reported for straight and bifurcating vessels. The Locally Conservative Taylor Galerkin method used in the present study is extensively tested previously for fluid flow, and a detailed discussion on the accuracy of the method is provided in references [10, 11]. Thus, no further validation for accuracy is reported here for the sake of brevity. The fluid properties used for the simulations are summarized in Table 3. The fluid motion is generated by applying an inlet pressure signal to the first node of the domain. It should be recollected that other primitive variables at the inlet and exit are computed via the characteristic variables. This is the more natural way of determining the boundary conditions at the inlet and exit of the domain. The inlet temperature of the fluid is set at 37°C to reflect the human body temperature. The external pressure acting on the wall is taken equal to zero.

4.1 Straight vessels

4.1.1 Constant inner wall temperature

In order to check the behaviour of the method, a simple problem of straight tube with constant inlet temperature is considered first. In this case the inner wall temperature is assumed to be constant in space and time (T_w=35.3°C). All the parameters related to the straight tube problem are listed in Table 4. All the variables are monitored at the mid point of the segment.

The effects of a constant and pulsatile flow on temperature field are compared in Figure 2. The periodical signal is characterized by a pressure pulse with a width equal to $0.43s$. For both cases, pressure, area, velocity and temperature evolutions in time at mid point are shown in Figure 2. As discussed in section 3, A, u and p waveforms propagate in time along the tube at an

intrinsic wave speed velocity of c, while T is transported by velocity field u. For the case in which velocity is constant, the temperature reaches an expected steady and stable value, slightly lower than the inlet temperature due to lower inner wall temperature. With a periodic pressure pulse, the behaviour is completely different. While there are no surprises in the velocity, area and pressure value distributions, very small local oscillations in temperature are observed. This is inline with the variations in velocity values. When the velocity value peaks, it introduces an reduced cooling effect resulting in a slightly higher temperature than average temperature. However, when the velocity value is reduced, increased flow stagnation decreases the temperature value. This decrease in temperature is a result of enhanced heat transfer between the fluid and the wall due to reduced velocity. Such behaviour continues according to the prescribed pressure pulse in a cyclic manner as shown in Figure 2.

To investigate the effects of reflections on heat transfer, three cases with prescribed exit reflection coefficients are examined next. A case without reflection (R_t=0), partial reflection (R_t=0.5) and total reflection (R_t=1) are studied. The results are shown in Figure 3. As seen, the flow and heat transfer results with zero reflection coefficient are not different from the one discussed previously. However, as the wave reflection is introduced at the exit the reverse wave produces a strong cooling effect on the fluid. This is due to the fact that the reflected flow waves increase the fluid contact duration with the cold inner wall surface. This cooling effect is particularly pronounced when the wave is fully reflected.

4.1.2 Convective inside/outside wall conditions

In this problem, the inner wall surface temperature is allowed to vary in time and space. Thus, the heat conduction model for the surrounding wall material is now invoked. The model parameters and the outside conditions are reported in Table 5. All the remaining parameters for the study are same as the previous section.

To study the influence of the external heat transfer coefficient, the temperature is monitored at three points at the mid cross section of the vessel as shown in Figure 4. To clearly quantify the influence of external heat transfer coefficient, all other parameters, including internal wall heat transfer coefficient are fixed as given by Tables 3, 4 and 5. In Figure 4, temperature evolutions at points 1,2 and 3 are shown for different heat transfer coefficients. As seen the cooling effect is enhanced as the heat transfer coefficient is increased. Also, the temperature pattern with respect time in the fluid is very similar to the previously experienced pattern. However, the difference here is that the reduction in temperature here is controlled by external heat transfer coefficient at the outer surface of the vessel. In all cases, the time taken for the temperature to reach a steady state is much higher than the previous, constant wall temperature example. Similar to the previous problem, the temperature of the fluid shows minor oscillatory behaviour representing the pulsatile motion of the fluid. This behaviour is especially enhanced at higher external heat transfer coefficient values.

Next, we investigate the effect of wall properties on heat transfer. A combination of wall properties may be represented through the material parameter β. However, the wall thickness (h),

unstressed area (A_o) and Young's modulus of the material (E) may also be changed along with β. Apart from β, other parameters used in the calculations remain the same. The effect of wall thickness and corresponding β variation on flow and heat transfer is shown in Figure 5. As seen both the velocity and temperature exhibits pulsatile behaviour. It is clear that when β decreases, the decreased resistance to flow increases the average flow speed. The average fluid temperature also slightly decreases with β value. However, the peak temperature values slightly increase with decrease in β values. This may be due to the increased flow speed and reduced contact time between fluid and cold wall. The pulsating behaviour of the temperature remains the same as the problem with constant inner wall temperature.

4.2 Vessel branching

In this section, the effect of introducing a bifurcation is studied. The system considered includes three tubes that are linked by means of a bifurcation. Each of them has a length equal to 10 cm. Monitoring points (4 and 5) are positioned at the mid point the segments as shown in Figure 6. The tube associated with the point 5 has an unstressed area (A_o) that is equal to half of unstressed area of point 4. A comparison is carried out against a straight tube of identical total length with monitoring points at 6 and 7 as shown in Figure 6. In the straight tube case, the unstressed area is equal to the area at point 4. The heat transfer results are also shown in Figure 6. As expected, the bifurcation modifies the velocity field slightly. After the branching, the velocity signal is slightly attenuated. Both the velocity amplitude values, before and after bifurcation, have been reduced in comparison to the straight tube value. While there is no significant difference in heat transfer between parent vessel of the bifurcation and straight tube, a reduction in temperature is observed in the daughter vessels. This is the result of smaller velocity in comparison to the straight tube and also due to increase in the ratio between surface area and cross sectional area of daughter vessels.

5 Concluding remarks

A one-dimensional thermo-fluid model for an elastic tube and tube network has been developed and numerically tested. The novel aspect of the work is in the introduction of a comprehensive model for energy transport. Hence, the present model can predict the influence of the flow rate, and the pressure as well as that of the cross-sectional area on the temperature. The influence of structural properties of the vessel wall and various other properties on heat transfer has been investigated. Due to the fact that the transport velocity for the temperature is the velocity of the fluid, any parameter that influences the velocity also influences the fluid temperature. Although the inlet fluid temperature is assumed to be constant, the temperature down stream follows a pattern inline with the pulsatile pattern of flow velocity. It is conclusively shown that decrease in the material parameter β decreases the average fluid temperature. The effect of bifurcation with smaller daughter vessels increases the cooling effect. This is due to the increase in surface area to cross sectional area ratio and reduction in velocity in comparison to an equivalent straight tube.

Acknowledgements

The authors would like to thank E. Boileau and Prof. V. Verda for their support during the development of the code.

References

[1] A. Avolio, Multi-branched model of the human arterial system. *Medical and Biological Engineering and Computing*, 18, 709-718, 1980.

[2] N. Stergiopulos, D.F. Young and T.R. Rogge, Computer simulation of arterial flow with applications to arterial and aortic stenoses, *Journal of Biomechanics*, 25, 1477-1488, 1992.

[3] L. Formaggia, F. Nobile and A. Quarteroni, A one dimensional model for blood flow: application to vascular prosthesis. In Mathematical Modeling and Numerical Simulation in Continuum Mechanics, Babuska I, Miyoshi T, Ciarlet PG (eds), *Lecture Notes in Computational Science and Engineering*, Springer: Berlin, 2002.

[4] J. Wan, B. Steele, A.A. Spicer, S. Strohband, G.R. Feijoo, T.F.R. Hughes and C.A. Taylor, A one-dimensional finite element method for simulation-based medical planning for cardiovascular disease, *Computer Methods in Biomechanics and Biomedical Engineering*, 5, 195-206, 2002.

[5] S.J. Sherwin, L. Formaggia, J. Peiró, and V. Franke, Computational modelling of 1D blood flow with variable mechanical properties and its application to the simulation of wave propagation in the human arterial system, *International Journal for Numerical Methods in Fluids*, 43, 673-700, 2003.

[6] S.A. Urquiza, P.J. Blanco, M.J. Vénere and R.A. Feijóo, Multidimensional modelling for the carotid artery blood flow, *Computer Methods in Applied Mechanics and Engineering*, 195, 4002-4017, 2006.

[7] J. Alastruey, K.H. Parker, J. Peiró, S.M. Byrd and S.J. Sherwin, Modelling the circle of willis to assess the effects of anatomical variations and occlusions on cerebral flows. *Journal of Biomechanics*, 40, 1794-1805, 2007.

[8] B.N. Steele, M.S. Olufsen and C.A.Taylor, Fractal network model for simulating abdominal and lower extremity blood flow during resting and exercise conditions, *Computer Methods in Biomechanics and Biomedical Engineering*, 10, 39-51, 2007.

[9] J.J. Wang and K.H Parker, Wave propagation in a model of the arterial circulation, *Journal of Biomechanics*, 37, 457-470, 2004.

[10] J.P. Mynard and P. Nithiarasu, A 1D arterial blood flow model incorporating ventricular pressure, aortic valve and regional coronary flow using locally conservative Galerkin (LCG) method, *Communications in Numerical Methods in Engineering*, 24, 367-417, 2008.

[11] K. Low, R. van Loon, I. Sazonov, R. L. T. Bevan and P. Nithiarasu, An improved baseline model for a human arterial network to study the impact of aneurysms on pressure-flow waveforms, *International Journal for Numerical Methods in Biomedical Engineering*, 28, 1224-1246, 2002.

[12] Peng Chen, Alfio Quarteroni and Gianluigi Rozza, Simulation-based uncertainty quantification of human arterial network hemodynamics, *International Journal for Numerical Methods in Biomedical Engineering*, 29, 698-721, 2013.

[13] J. P. Mynard, M. R. Davidson, D. J. Penny and J. J. Smolich, A simple, versatile valve model for use in lumped parameter and one-dimensional cardiovascular models, *International Journal for Numerical Methods in Biomedical Engineering*, 28, 626-641, 2012.

[14] Blanco, P.J., Trenhago, P.R., Fernandes, L.G. and Feijóo, R.A., On the integration of the baroreflex control mechanism in a heterogeneous model of the cardiovascular system. *International Journal for Numerical Methods in Biomedical Engineering*, 28, 412-433, 2012.

[15] Blanco, P. J., Leiva, J. S. and Buscaglia, G. C., A black-box decomposition approach for coupling heterogeneous components in hemodynamics simulations,*International Journal for Numerical Methods in Biomedical Engineering*, 29, 408-427, 2013.

[16] Itu, L., Sharma, P., Kamen, A., Suciu, C. and Comaniciu, D., Graphics processing unit accelerated one-dimensional blood flow computation in the human arterial tree. *International Journal for Numerical Methods in Biomedical Engineering*, 29, 1428-1455, 2013.

[17] Yang, J. and Wang, Y., Design of vascular networks: A mathematical model approach, *International Journal for Numerical Methods in Biomedical Engineering*, 29, 515-529, 2013.

[18] Alastruey, J., Hunt, A. A. E. and Weinberg, P. D., Novel wave intensity analysis of arterial pulse wave propagation accounting for peripheral reflections. *International Journal for Numerical Methods in Biomedical Engineering*,30, 249-279, 2014.

[19] R.B. Roemer, Engineering aspects of hyperthermia therapy, *Annual Reviews Biomedical Engineering*,1, 347 - 376, 1999.

[20] P. Wust, B. Hildebrandt, G. Sreenivasa, B. Rau, J. Gellermann, H. Riess, R. Felix, P.M. Schlag, Hyperthermia in combined treatment of cancer, *Lancet Oncology*, 3, 487-497, 2002.

[21] Tahar Loulou and Elaine P. Scott, Thermal dose optimisation in hyperthermia treatment by using the conjugate gradient method, *Numerical Heat Transfer, Part A: Applications*, 42, 661-683, 2002.

[22] Nazia Afrin, Jianhua Zhou, Yuwen Zhang, D. Y. Tzou and J. K. Chen, Numerical Simulation of Thermal Damage to Living Biological Tissues Induced by Laser Irradiation Based on a Generalized Dual Phase Lag Model, *Numerical Heat Transfer, Part A: Applications*, 61, 483-501, 2012.

[23] O.I. Craciunescu and S.T. Clegg, Pulsatile blood flow effects on temperature distribution and heat transfer in rigid vessels, *Transactions of ASME, Journal of Biomechanical Engineering*, 123, 500-505, 2001.

[24] H. Ying, L. Hao and H. Ryutaro, A one-dimensional thermo-fuid model of blood circulation in the human upper limb, *International Journal of Heat and Mass Transfer*, 47, 2735-2745, 2004.

[25] P. Nithiarasu, A simple locally conservative Galerkin (LCG) finite element method for transient conservation equations, *Numerical Heat Transfer, Part B Fundamentals*, 46, 357 - 370, 2004.

[26] C.G. Thomas and P. Nithiarasu, An element-wise, locally conservative Galerkin (LCG) method for solving diffusion and convection-diffusion problems, *International Journal for Numerical Methods in Engineering*, 73, 642-664, 2008.

[27] S.J. Sherwin, V. Franke, J. Peiró and K. Parker, One-dimensional modelling of a vascular network in space-time variables, *Journal of Engineering Mathematics*,47, 217-250, 2003.

[28] L. Formaggia, F. Nobile, A. Quarteroni, and A. Veneziani, Multiscale modelling of the circulatory system: a preliminary analysis, *Computing and Visualization in Science*, 2, 75-83, 1999.

[29] M.S. Olufsen, C.S. Peskin, W.Y. Kim, E.M. Pedersen, A. Nadim and J. Larsen, Numerical simulation and experimental validation of blood flow in arteries with structured-tree outflow conditions. *Annals of Biomedical Engineering*, 28, 1281-1299, 2000.

[30] C. Hirsch, Numerical Computation of Internal and External Flows, *Computational Method for Inviscid and Viscous Flows, vol. 2.* Wiley: Chichester, U.K., 1990.

[31] M. Anliker, R.L. Rockwell and E. Ogden, Nonlinear analysis of flow pulses and shock waves in arteries. Part i: derivation and properties of mathematical model. *Zeitschrift f¨ur Angewandte Mathematik und Physik (ZAMP)*, 22, 217-246, 1971.

[32] K.W. Thompson, Time dependent boundary conditions for hyperbolic systems, *Journal of Computational Physics*, 68, 1-24, 1887.

[33] G.H. Golub and C.F. Van Loan, *Matrix Computations*, John Hopkins University Press: Baltimore, MD, 1996.

Density of fluid, ρ (g/cm^3)	1.06
Viscosity of fluid, μ $(poise)$	$3.5\text{x}10^{-2}$
Thermal conductivity of fluid, k $(W/cm^{\circ}\text{C})$	0.05
Specific heat of fluid, c_p $(J/g^{\circ}\text{C})$	3.9
Inner wall heat transfer coefficient, h_{in} $(W/cm^{2\circ}\text{C})$	0.01

Table 3: Fluid parameters and properties used in simulations.

Poisson's ratio, σ	0.5
Unstressed area, A_0 (cm^2)	1.0
Material wall parameter, β $(dyne/cm^2)$	2.26974x10^5
Wall thickness, h (cm)	0.05
Tube length, L (cm)	20
Finite element size, l_e (cm)	2.0x10^{-2}

Table 4: Geometrical and material properties of the vessel used.

Solid wall density, ρ_s (g/cm^3)	1.30
Solid wall thermal conductivity, k_s $(W/cm$ °C)	0.075
Solid wall specific heat, c_{ps} $(J/g$ °C)	3.0
Outside atmosphere temperature, T_{ext} (°C)	20.0
Outside wall heat transfer coefficient, $h_{ext}(W/cm^2$ °C)	0.001 - 0.01

Table 5: Solid parameters and the outside conditions.

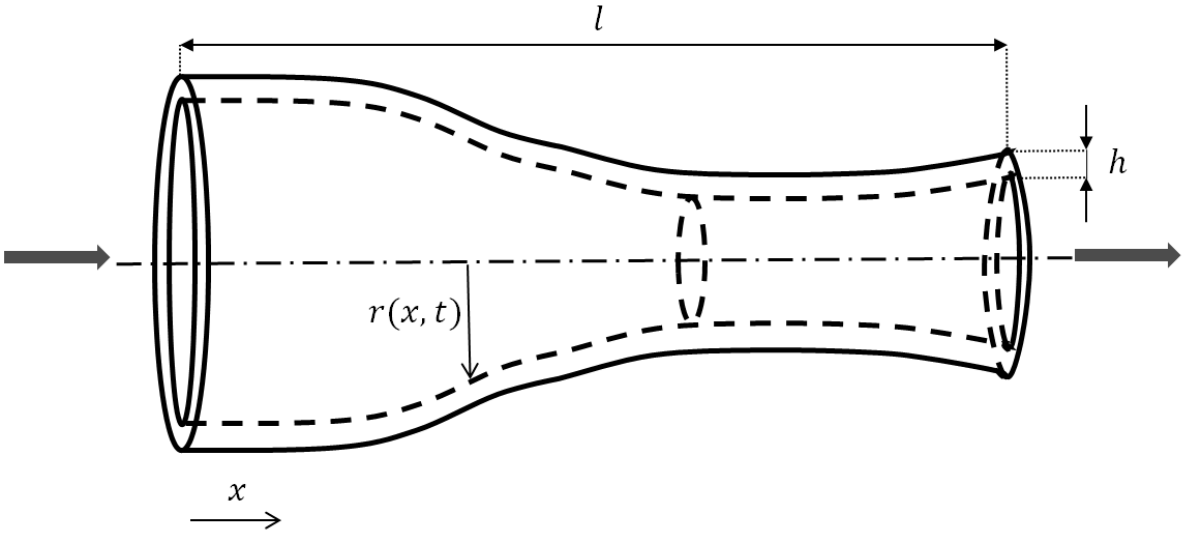

Figure 1: Schematic representation of flow and energy transport in a flexible tube.

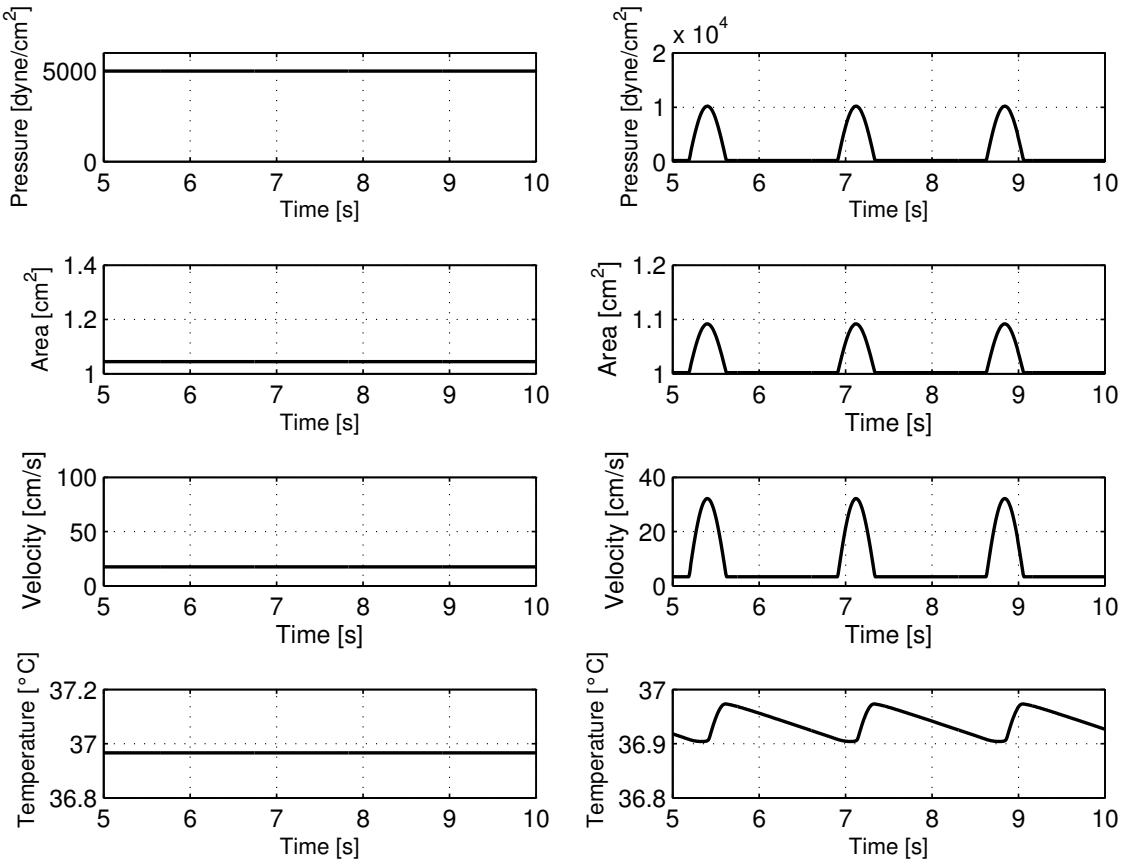

Figure 2: Flow and heat transfer in a flexible tube with a constant inner wall temperature. Pressure, area , velocity and temperature variations for constant (left) and pulsating (right) pressure inputs.

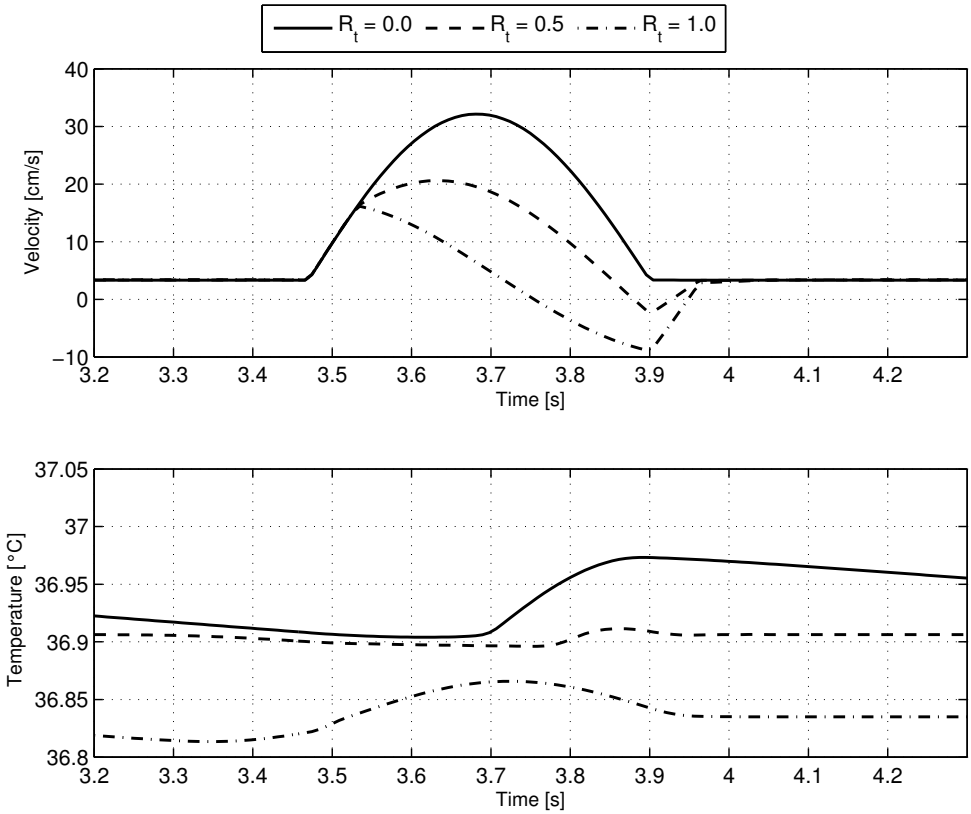

Figure 3: Flow and heat transfer in a flexible tube with a constant inner wall temperature. Effects of reflections on velocity and temperature.

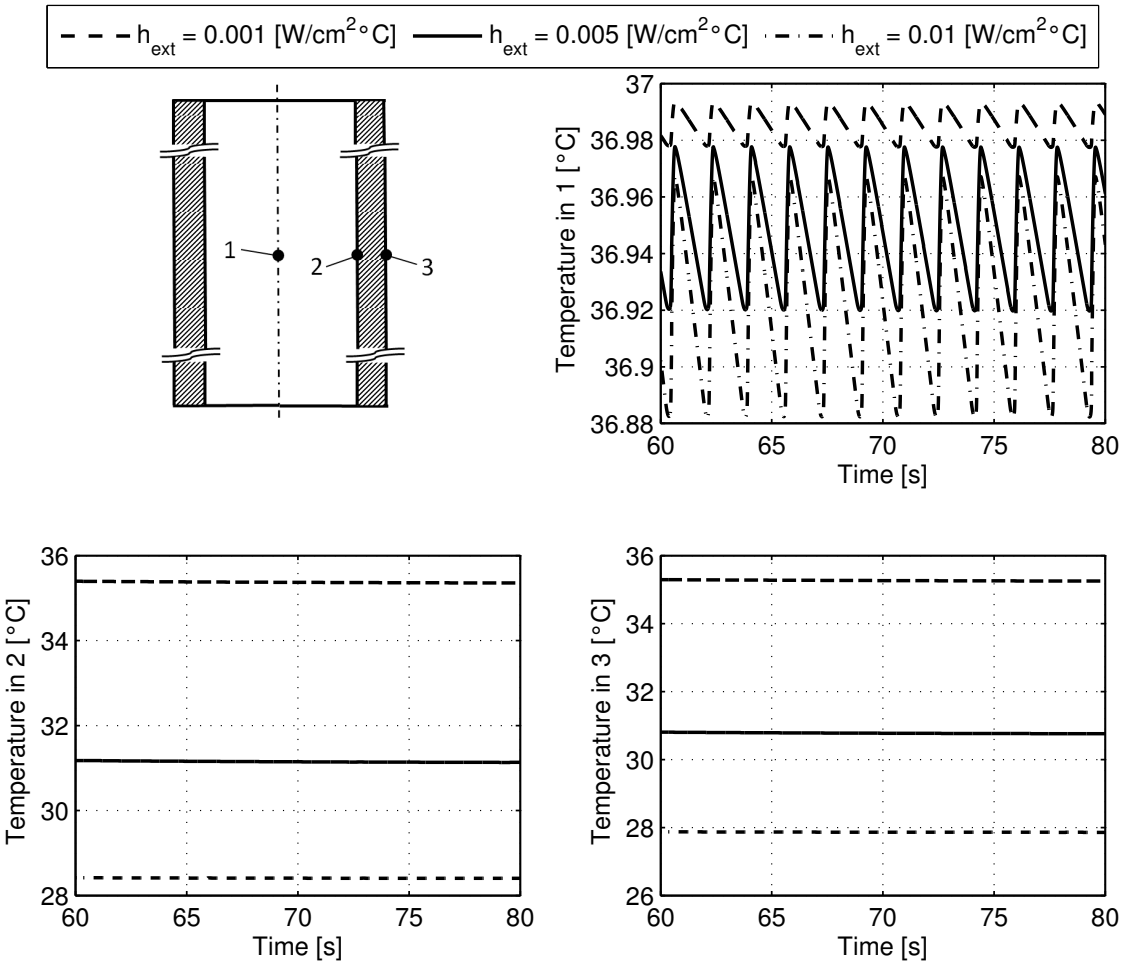

Figure 4: Flow and heat transfer in a flexible tube with a convective wall conditions. Effect of h_{ext} on temperature at points 1 (top right), 2 (bottom left) and 3 (bottom right)

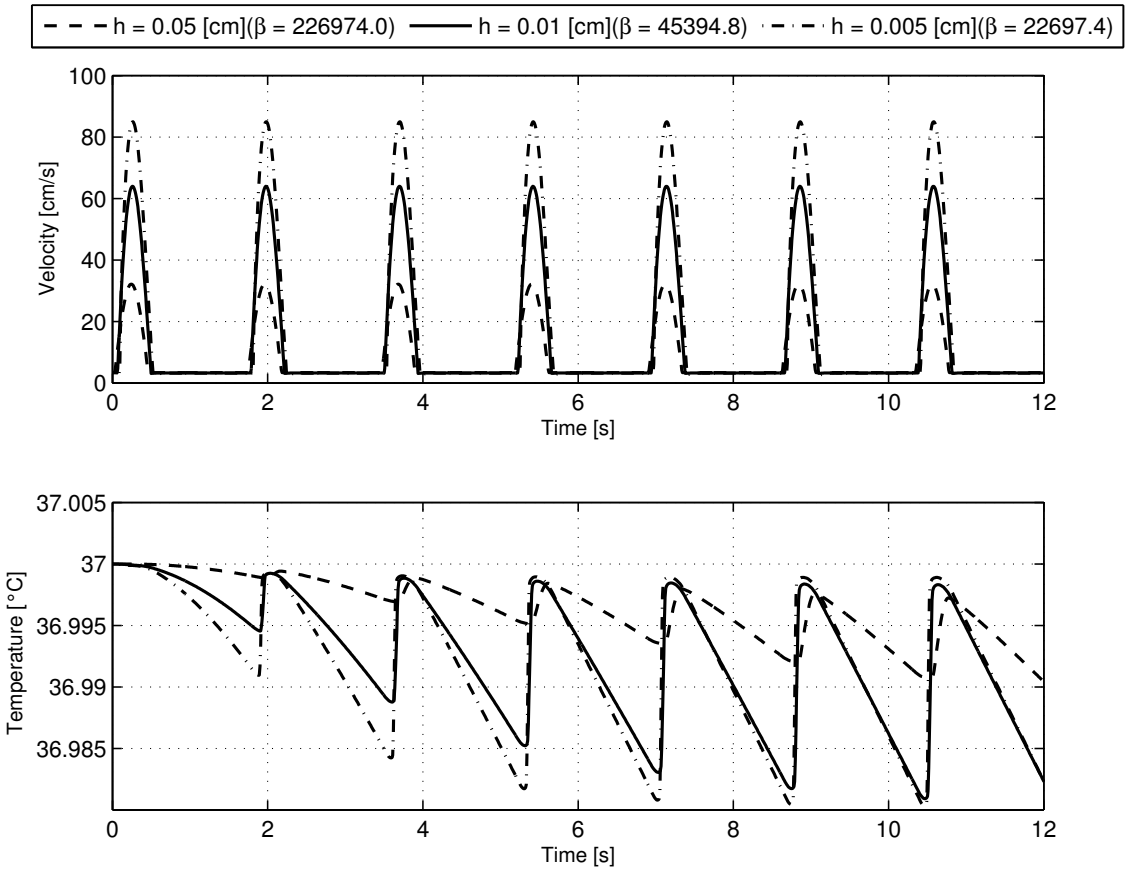

Figure 5: Flow and heat transfer in a flexible tube with a constant inner wall temperature. Effects of wall thickness (β) on fluid velocity and temperature.

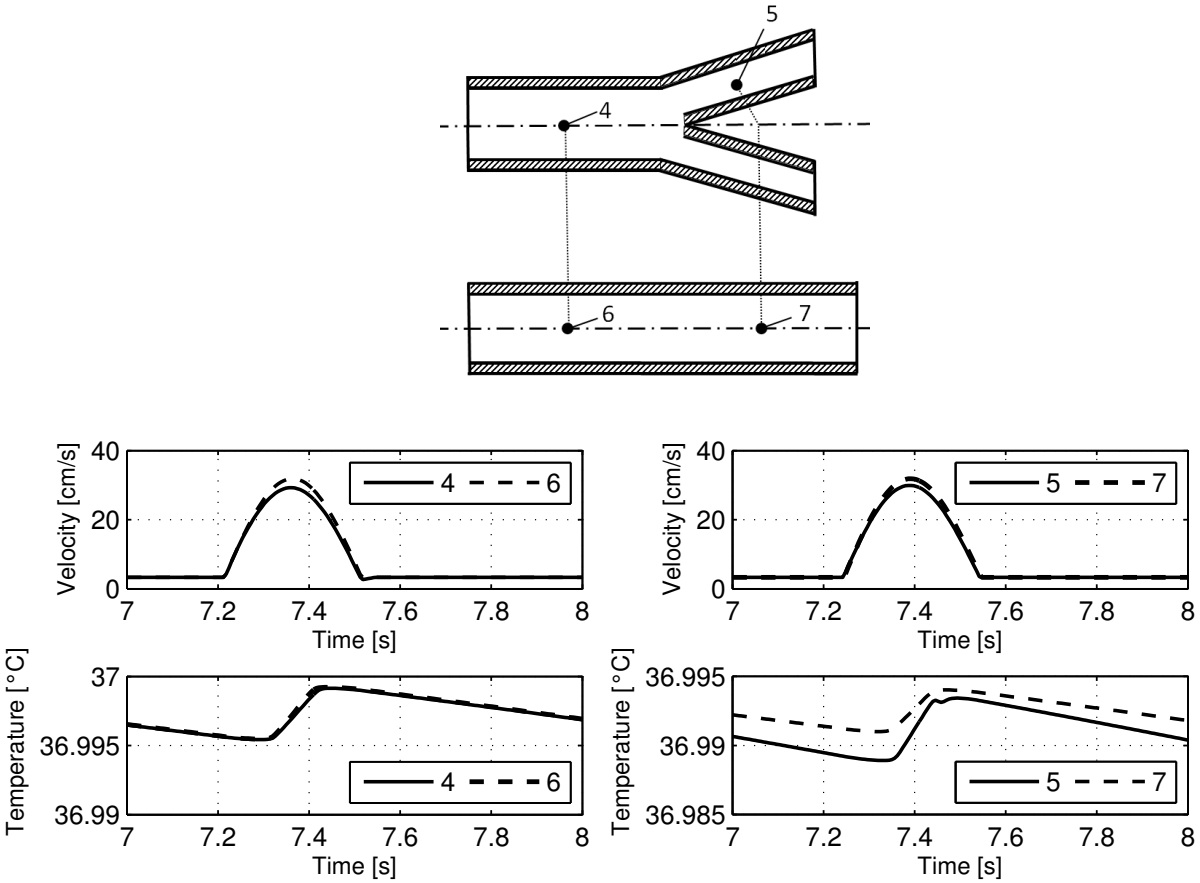

Figure 6: Flow and heat transfer in a bifurcating vessel with convective wall conditions. Velocity and temperature in a bifurcation